Journal of Physics: Conference Series

PAPER • OPEN ACCESS

Dynamic shear behaviour of truss towers for wind turbines

To cite this article: A Gesualdo *et al* 2018 *J. Phys.: Conf. Ser.* **1141** 012078

IOP Conf. Series: Journal of Physics: Conf. Series 1141 (2018) 012078 doi:10.1088/1742-6596/1141/1/012078

Dynamic shear behaviour of truss towers for wind turbines

A Gesualdo[1], **M Guadagnuolo**[2] **and F Penta**[3]
[1]*Department of Structures for Engineering and Architecture, University of Naples Federico II, Naples, Italy*
[2]*Department of Architecture and Industrial Design, University of Campania Luigi Vanvitelli, Aversa (CE), Italy*
[2]*Department of Industrial Engineering, University of Naples Federico II, Naples, Italy*

E-mails: {gesualdo, penta}@unina.it, mariateresa.guadagnuolo@unicampania.it

Abstract. The global interest in renewable energy sources has increased the attention to the manufacturing of wind turbine towers, since they are largely diffused in seismic areas too. Different types of towers have been produced in recent years. Among them, the truss structures assure a reduced mass and the modular characteristics necessary for easy transportation. Reduced costs of production, installation and maintenance are typical of these structures. Nonlinear dynamics is an efficient framework to analyze structures subjected to variable actions, i.e. to assess the seismic safety of wind turbine towers in case of earthquake actions. This study outlines a procedure to evaluate the post-elastic behavior of truss towers for wind turbines. Rigid-plastic behaviour is taken into account to develop approximate solutions for the problem of a tower modeled as a vertical cantilever beam and subjected to harmonic base motion. A comparison with the results of a finite element model is proposed.

1. Introduction

The need of renewable energy production has enhanced the construction of eolian parks, i.e. sets of modern wind turbine [1]. Several of these parks have been realized in seismic areas, like those built in Irpinia, a region of Southern Italy devastated by a strong earthquake in 1980. Nonlinear dynamics is a reliable tool to examine the effects of earthquake actions on these structures [2].

In general when the elastic response can be disregarded and micromechanical behaviour involves complex experimental tests [3], rigid-plastic approximations, i.e. constitutive and structural models with sufficient accuracy and low numerical complexities are useful [4, 5]. A limiting aspect of the rigid-plastic model is linked to the numerical stability of the derived computer methods, due to the instantaneous jump of stiffness between zero and infinite. The model presented in the following sections overcomes this last limit, although plastic shear models are less diffused than the rigid-plastic bending ones. Despite the limited use in dynamic problems, nevertheless the procedures involve low computational competence and limited number of mechanical parameters, i.e. the yield characteristics [6, 7]. Simple relationships are derived between the strength of the structure and parameters useful for design purposes [8].

---

[1] Via Claudio 21, 80125 Napoli, Italy.
[2] Abazia di San Lorenzo, Via San Lorenzo 1, 81031 Aversa (CE), Italy.
[3] Piazzale Tecchio 80, 80125 Napoli, Italy

A large amount of literature now exists for the dynamic plastic bending response of structural elements, both steel and reinforced concrete structures. Bending hinges represent in fact general response characteristics of several structural elements under transverse load [9, 10]. In both the bending and shear problems the important question is linked to the localization and extension of plastic hinges [11, 12]. Closed solution of the problem have been developed with the classical tools of numerical analysis like the linear complementarity [13, 14], while different approaches involving discretization of the structure into a finite number of mass points [15] have been recently attempted.
The single-degree-of-freedom model provides a preliminary assessment of the structure and a good estimation of the response mode, which is normally responsible for overall structural failure [16, 17]. The rigid-plastic cantilever beam can be in fact a simple structural scheme to clarify the behaviour of more complex structures [18, 19] and to verify the accuracy of the numerical methods in a nonlinear dynamic analysis [20, 21]. In some cases, like that of rigid bodies, efficient schematizations are needed to solve complex dynamic problems [22, 23]. In the case of wind turbine towers a strong analogy with the cantilever beam can be recognized, so that the single degree of freedom provides useful results, also in the cases where there is a variation of strength and mass over the height. In general, pulses that occur during earthquakes have qualitative and quantitative characteristics that can adequately be approximated by specific functional expressions obtained by means of wavelet analysis [24]. Several strong ground motions contain in fact an acceleration pulse responsible for most of the inelastic deformations of structures. That acceleration pulse has been determined in some cases analyzing the main strong earthquakes occurred in the last 50 years [25]. The accurate choice of harmonic pulses to represent the ground motion are necessary to evaluate elastic and inelastic response spectra [26]. Sensitive analyses of responses due to different simple pulse shapes due to elastic and inelastic behaviour has shown that local site effects on structures can be modelled with an appropriate choice of the pulse [27, 28, 29]. These considerations are the basis of the numerical analysis performed, since the harmonic pulse can be a suitable representation of near-fault ground motions [30].

In this paper approximate solutions for rigid-plastic shear response of structures subjected to harmonic base pulse is presented, implemented in a numerical procedure on purpose developed. The results of the step by step solution of the general nonlinear dynamic problem are shown in form of time histories. The fundamental equations of the problem [31] are based on the rigid-plastic constitutive model and applied to the structure of a truss tower for a wind turbine considered like a cantilever beam subjected to harmonic forcing motion of the base support. The failure is assumed depending on the formation shear hinges and the results are expressed in general terms for application to real cases.

2. The nonlinear dynamic problem

Simplified constitutive models are of limited validity if applied to structures subjected to short duration and high intensity loading, on the contrary they are useful in case of estimate of major deformations due to very large dynamic loads [32, 33]. This estimation can be successively refined to include the initially neglected aspects. In what follows geometry changes are small and the yield stress is assumed to be independent on the strain rate. Reference is made to the elastic perfectly plastic body in Fig. 1, where:

$\partial\Omega = \partial\Omega_t \bigcup \partial\Omega_u$:	total boundary of the body Ω and $\partial\Omega_t \bigcap \partial\Omega_u = \varnothing$
$\partial\Omega_t$, $\partial\Omega_u$:	free and constrained boundary of the body Ω
$\lambda(t)\ \boldsymbol{t}(\boldsymbol{x})$:	surface loads on the free boundary $\partial\Omega_t$
$\lambda(t)\ \boldsymbol{b}(\boldsymbol{x})$:	body forces in Ω
$\dot{\boldsymbol{u}}_g(\boldsymbol{x},t)$:	assigned velocity vector and $\dot{\boldsymbol{u}}(\boldsymbol{x},0) = \boldsymbol{0}$ on $\partial\Omega_u$
$\lambda(t)$:	time dependent load multiplier function.

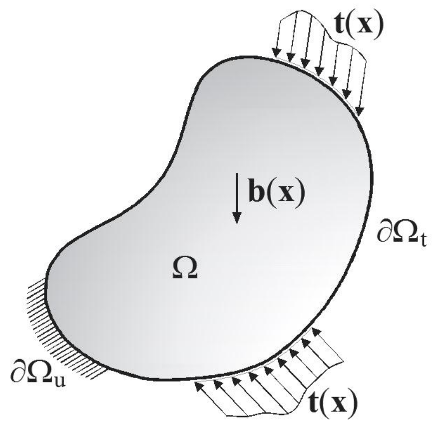

Fig. 1 The elastic perfectly plastic body

The solution of the elastoplastic problem gives the strain rate $\dot{\boldsymbol{E}}(\boldsymbol{x},t)$ and velocity fields $\dot{\boldsymbol{u}}(\boldsymbol{x},t)$ satisfying the kinematical admissibility conditions and the stress field $\boldsymbol{T}(\boldsymbol{x},t)$ equilibrated with the applied loads $\lambda(t)\,\boldsymbol{t}(\boldsymbol{x})$, $\lambda(t)\,\boldsymbol{b}(\boldsymbol{x})$ and the inertial forces $-\mu(\boldsymbol{x})\ddot{\boldsymbol{u}}^*(\boldsymbol{x},t)$, being $\mu(\boldsymbol{x})$ the mass density function. In the following the approximate response field [34] is assumed in the form:

$$\dot{\boldsymbol{u}}^*(\boldsymbol{x},t) = \boldsymbol{\Phi}(\boldsymbol{x})\,L(t) \tag{1}$$

with:

$\dot{\boldsymbol{u}}^*(\boldsymbol{x},t)=\dot{\boldsymbol{u}}_g(\boldsymbol{x},t)$ on $\partial\Omega_u$; $\dot{\boldsymbol{u}}^*(\boldsymbol{x},t)=\boldsymbol{0}$ in Ω and $\partial\Omega_t$

where the assigned vector $\boldsymbol{\Phi}(\boldsymbol{x})$ depends on the initial position only and $L(t)$ is an unknown scalar function of the time [35] to be determined. The difference between the real stress field and the approximate one is in balance with the variation of the associate force fields, reduced to the difference between the inertial forces. The problem solution does not require that $\boldsymbol{T}^*(\boldsymbol{x},t)$ and $\dot{\boldsymbol{E}}^*(\boldsymbol{x},t)$ are associated by the plastic law, so that the stress field is dynamically admissible with respect to the D'Alembert principle. Applying the principle of virtual power

$$\int_\Omega \mu(\ddot{\boldsymbol{u}}-\ddot{\boldsymbol{u}}^*)\cdot(\dot{\boldsymbol{u}}-\dot{\boldsymbol{u}}^*)\,d\Omega+\int_\Omega(\boldsymbol{T}-\boldsymbol{T}^*)\cdot(\dot{\boldsymbol{E}}-\dot{\boldsymbol{E}}^*)\,d\Omega=0 \tag{2}$$

and stating

$$\Delta(t)=\frac{1}{2}\int_\Omega \mu(\dot{\boldsymbol{u}}-\dot{\boldsymbol{u}}^*)\cdot(\dot{\boldsymbol{u}}-\dot{\boldsymbol{u}}^*)\,d\Omega \tag{3}$$

the first derivative of $\Delta(t)$ is calculated:

$$\frac{d\Delta}{dt}=\int_\Omega \mu(\ddot{\boldsymbol{u}}-\ddot{\boldsymbol{u}}^*)\cdot(\dot{\boldsymbol{u}}-\dot{\boldsymbol{u}}^*)\,d\Omega \tag{4}$$

In view of (4) and (2) it has:

$$\frac{d\Delta}{dt}=-\int_\Omega(\boldsymbol{T}-\boldsymbol{T}^*)\cdot(\dot{\boldsymbol{E}}-\dot{\boldsymbol{E}}^*)\,d\Omega=0$$

thus:

$$\frac{d\Delta}{dt} = -\int_\Omega \left[(\boldsymbol{T}-\boldsymbol{T}^*)\cdot \dot{\boldsymbol{E}}^* + (\boldsymbol{T}^*-\boldsymbol{T})\cdot \dot{\boldsymbol{E}}^* \right] d\Omega = \int_\Omega \left[(\boldsymbol{T}^*-\boldsymbol{T})\cdot \dot{\boldsymbol{E}} + (\boldsymbol{T}-\boldsymbol{T}^*)\cdot \dot{\boldsymbol{E}}^* \right] d\Omega \tag{5}$$

The stress field $\boldsymbol{T}$ and the strain rate $\dot{\boldsymbol{E}}$ are associated through the plastic flow rule, while $\boldsymbol{T}^*$ satisfies the plasticity condition. The Drucker's stability postulate holds:

$$(\boldsymbol{T}-\boldsymbol{T}^*)\cdot \dot{\boldsymbol{E}} \geq 0\,. \tag{6}$$

In the regions where $\dot{\boldsymbol{E}}^*(\boldsymbol{x},t) \neq \boldsymbol{0}$, the generalized stress field $\boldsymbol{T}^*_{\dot{\boldsymbol{E}}^*}$ associated to $\dot{\boldsymbol{E}}^*$ through the flow rule satisfies the plasticity condition:

$$(\boldsymbol{T}^*_{\dot{\boldsymbol{E}}^*}-\boldsymbol{T})\cdot \dot{\boldsymbol{E}}^* \geq 0\,. \tag{7}$$

By Drucker's stability postulate the equation (5) may therefore be put in the form:

$$\frac{d\Delta}{dt} = \int_\Omega \left[(\boldsymbol{T}^*-\boldsymbol{T})\cdot \dot{\boldsymbol{E}} + (\boldsymbol{T}-\boldsymbol{T}^*)\cdot \dot{\boldsymbol{E}}^* \right] d\Omega = \tag{8.a}$$

$$= \int_\Omega (\boldsymbol{T}^*-\boldsymbol{T})\cdot \dot{\boldsymbol{E}}\, d\Omega + \int_\Omega (\boldsymbol{T}-\boldsymbol{T}^*_{\dot{\boldsymbol{E}}^*})\cdot \dot{\boldsymbol{E}}^* d\Omega + \int_\Omega (\boldsymbol{T}^*_{\dot{\boldsymbol{E}}^*}-\boldsymbol{T}^*)\cdot \dot{\boldsymbol{E}}^* d\Omega \leq \tag{8.b}$$

$$\leq \int_\Omega (\boldsymbol{T}^*_{\dot{\boldsymbol{E}}^*}-\boldsymbol{T}^*)\cdot \dot{\boldsymbol{E}}^* d\Omega = \Gamma(t) \;\Rightarrow\; \Gamma(t) \geq 0 \tag{8.c}$$

where the first and the second integral in 8(b) are both less or equal to zero, hence the last term in (8.c) results non-negative, so that:

$$\frac{d\Delta}{dt} \leq \Gamma(t)\,. \tag{9}$$

The integration of the previous relation from 0 to time *t* gives the approximation measure $\Delta(t)$:

$$\Delta(t) \leq \Delta^+(t) = \int_0^t \Gamma(t)\, dt\,. \tag{10}$$

The maximum value Δ_m of the non decreasing time function $\Delta^+(t)$ is $\Delta^+(T)$, being *T* the duration of the external forcing function. The function $L(t)$ satisfies the initial conditions:

$$L(0) = 0\,. \tag{11}$$

Due to the condition $\dot{\boldsymbol{u}}^*(\boldsymbol{x},0) = 0$. If $\boldsymbol{\Psi}(\boldsymbol{x})$ is the vector involving the strain generalized components associated to modal vector $\boldsymbol{\Phi}(\boldsymbol{x})$, the acceleration $\ddot{\boldsymbol{u}}^*(\boldsymbol{x},t)$ and the strain rate $\dot{\boldsymbol{E}}^*$ are given by:

$$\ddot{\boldsymbol{u}}^*(\boldsymbol{x},t) = \boldsymbol{\Phi}(\boldsymbol{x})\dot{L}(t) \quad ; \quad \dot{\boldsymbol{E}}^*(\boldsymbol{x},t) = \boldsymbol{\Psi}(\boldsymbol{x})L(t) \tag{12}$$

The principle of virtual velocity gives:

$$\int_{S_L} \boldsymbol{p}(\boldsymbol{x},t)\cdot \dot{\boldsymbol{u}}^* dS + \int_\Omega [\boldsymbol{F}(\boldsymbol{x},t) - \mu \ddot{\boldsymbol{u}}^*]\cdot \dot{\boldsymbol{u}}^* d\Omega = \int_\Omega \boldsymbol{T}^*(\boldsymbol{x},t)\cdot \dot{\boldsymbol{E}}^*(\boldsymbol{x},t)\, d\Omega \tag{13}$$

that can be manipulated with reference to (1) and (12):

$$\int_{S_L} \boldsymbol{p}^T(\boldsymbol{x},t)\boldsymbol{\Phi}(\boldsymbol{x}) dS + \int_\Omega \boldsymbol{F}^T(\boldsymbol{x},t)\boldsymbol{\Phi}(\boldsymbol{x}) d\Omega =$$
$$= \dot{L}(t) \int_\Omega \mu(\boldsymbol{x})\boldsymbol{\Phi}^T(\boldsymbol{x})\boldsymbol{\Phi}(\boldsymbol{x}) d\Omega + \int_\Omega \boldsymbol{T}^*(\boldsymbol{x},t)\boldsymbol{\Psi}(\boldsymbol{x}) d\Omega$$

so that the function $L(t)$ can be evaluated by integration of the following function:

$$\dot{L}(t)=\frac{\int_{S_L}\boldsymbol{p}^T(\boldsymbol{x},t)\boldsymbol{\Phi}(\boldsymbol{x})dS+\int_{\Omega}\boldsymbol{F}^T(\boldsymbol{x},t)\boldsymbol{\Phi}(\boldsymbol{x})d\Omega-\int_{\Omega}\boldsymbol{T}^*(\boldsymbol{x},t)\boldsymbol{\Psi}(\boldsymbol{x})d\Omega}{\int_{\Omega}\mu(\boldsymbol{x})\boldsymbol{\Phi}^T(\boldsymbol{x})\boldsymbol{\Phi}(\boldsymbol{x})d\Omega}. \tag{14}$$

This method can be applied to pulse loads, with the two conditions that the tractions applied to $\partial\Omega_t$ are null and the initial velocities are prescribed over the whole structure at time $t=0$; therefore, no external forces do work on the structure.

3. Plastic shear behaviour of a cantilever beam

The single-degree-of-freedom (SDOF) model is a good schematization for the dynamic behaviour of various structure [36]. In particular the wind turbine towers can be easily represented by a cantilever beam supported at the base.

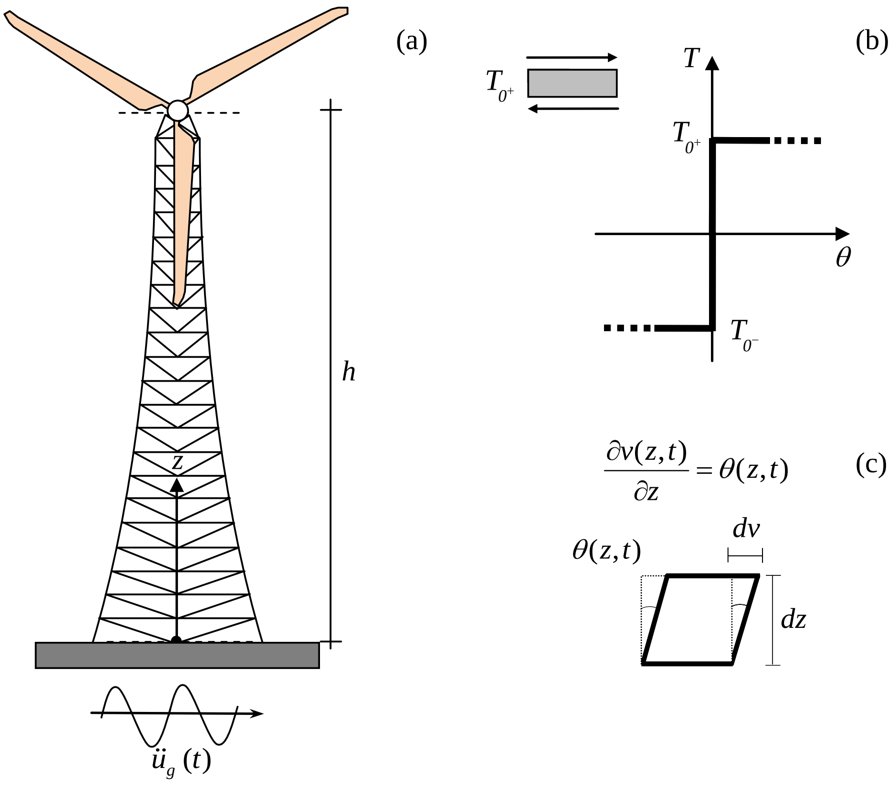

Fig. 2 Wind turbine tower geometry (a), rigid-plastic constitutive law (b) and shear strain representation (c)

As elsewhere shown [7] the rigid-plastic cantilever beam allows to develop a simplified approach to the nonlinear dynamic problem arising for sinusoidal excitation at the base of the tower. The problem is one-dimensional, so that parameters and relations developed in the previous section become scalar. In the model presented the Cartesian reference frame has the origin in the support section and the z axis coincident with the wind tower axis (Fig. 2a). The local yield kinematism corresponds to the activation of a shear hinge in which the total shear force $T(z,t)$ attains its bound value. The mechanical characteristics are shown in Fig. 2b and 2c, where:

$\mu(z)$: linear mass density of the tower
$u_g(t)$: horizontal motion of the supported section
$T(z,t)$: shear stress whose bounds are $T_{0^+}(z)$ and $T_{0^-}(z)$
$\theta(z,t)$: shear strain
h: total length of the tower.

The shear plastic constitutive relations are the following:

$$\begin{cases} \left[T(z,t)-T_{0^+}(z)\right]\left[T(z,t)+T_{0^-}(z)\right]\dot{\theta}(z,t)=0 \\ -T_{0^-}(z)\le T(z,t)\le T_{0^+}(z) \end{cases} \tag{15}$$

that is

$$\begin{array}{lll} -T_{0^-}<T<T_{0^+} & \dot{\theta}=0 \;\Rightarrow & \left[T-T_{0^+}\right]\dot{\theta}=0 \text{ and } \left[T+T_{0^-}\right]\dot{\theta}=0 \\ T=T_{0^+} & \dot{\theta}\neq 0 \;\Rightarrow & \left[T-T_{0^+}\right]\dot{\theta}=0 \\ T=-T_{0^-} & \dot{\theta}\neq 0 \;\Rightarrow & \left[T+T_{0^-}\right]\dot{\theta}=0. \end{array}$$

where the plastic strain rate $\dot{\theta}$ depends on the shear stress only. The dynamic equilibrium equation in the cross section at the z level involves the inertial forces only:

$$\frac{\partial T(z,t)}{\partial z}=\mu(z)\ddot{u}(z,t)=\mu(z)[\ddot{u}_g(t)+\ddot{v}(z,t)]. \tag{16}$$

where:

$$u(z,t)=u_g(t)+v(z,t), \tag{17}$$

is the absolute displacement and:

$$v(z,t)=\int_0^z \theta(x,t)dx=\int_0^z\int_0^t \dot{\theta}(x,\tau)d\tau\, dx \tag{18}$$

is the relative one. A plastic shear hinge occurs when the limit value of shear stress is reached. One or more shear hinges can be activated in the sections $z_1, z_2, ..., z_n$ during the plastic phase, and their abscissa varies according to the time. The kinematic compatibility states that the plastic strain rate is non null in the active hinges only:

$$\dot{\theta}(z,t)=\frac{\partial \dot{v}(z,t)}{\partial z}=\dot{v}'(z,t). \tag{19}$$

The relative displacement $v(z,t)$ in (18) can be deduced integrating (19) with respect to z and introducing the Heaviside function $H(z)$ ($H(z)=0$ for $z<0$, $H(z)=1$ *for* $z\ge 0$):

$$v(z,t)=\int_0^z v'(x,t)dx=\int_0^z \theta(x,t)dx=\int_0^h \theta(x,t)H(z-x)dx. \tag{20}$$

A double time derivation gives the relative acceleration $\ddot{v}(z,t)$:

$$\ddot{v}(z,t)=\int_0^z \ddot{\theta}(x,t)dx=\int_0^h \ddot{\theta}(x,t)H(z-x)dx \tag{21}$$

In case of only one shear hinge active the time dependent position is denoted with $z_0(t)$, so the relative displacement velocity and the plastic strain rate have the form:

$$\dot{v}(z,t) = \dot{v}_1(t)\, H[z - z_0(t)]$$

$$\dot{\theta}(z,t) = \dot{v}'(z,t) = \dot{v}_1(t)\ \delta[z - z_0(t)]$$

being $\delta[z - z_0(t)]$ the Dirac function relative to the plastic hinge position. The shear stress become:

$$T(z,t) = \ddot{u}_g(t)\int_h^z \mu(x)\,dx + \int_h^z \mu(x)\,\ddot{v}(x,t)dx = \ddot{u}_g(t)\int_h^z \mu(x)\,dx + \ddot{v}_1(t)\int_h^z \mu(x)\,H[x - z_0(t)]dx$$

The mass functions are:

$$m(z) = \int_h^z \mu(x)\,dx \quad ; \quad m_H[z, z_0(t)] = \int_h^z \mu(x)\,H[x - z_0(t)]\,dx \tag{22}$$

the time derivative of the second relation (22) gives:

$$\frac{\partial m_H[z, z_0(t)]}{\partial t} = -\mu(z)\,\dot{z}_0(t) H[z - z_0(t)] = -\dot{z}_0(t)\frac{\partial m_H[z, z_0(t)]}{\partial z}.$$

The shear stress and its derivatives in function of the masses are:

$$T(z,t) = \ddot{u}_g(t)\,m(z) + \ddot{v}_1(t)\,m_H[z, z_0(t)]$$

$$\frac{\partial T(z,t)}{\partial z} = \mu(z)\ddot{u}_g(t) + \ddot{v}_1(t)\frac{\partial m_H[z, z_0(t)]}{\partial z}$$
$$\frac{\partial T(z,t)}{\partial t} = m(z)\dddot{u}_g(t) + \dddot{v}_1(t)\,m_H[z, z_0(t)] - \dot{z}_0(t)\,\ddot{v}_1(t)\frac{\partial m_H[z, z_0(t)]}{\partial z}.$$

The approximation by the Taylor series of the shear stress is:

$$\begin{aligned} T(z_0 + dz_0, t + dt) = T(z_0, t) &+ \left\{ \mu(z_0)\,\ddot{u}_g(t) + \ddot{v}_1(t)\left.\frac{\partial m_H[z, z_0(t)]}{\partial z}\right|_{z=z_0} \right\} dz_o + \\ &+ \left\{ m(z_0)\,\dddot{u}_g(t) + \dddot{v}_1(t)\,m_H[z_0, z_0(t)] - \ddot{v}_1(t)\,\dot{z}_0(t)\left.\frac{\partial m_H[z, z_0(t)]}{\partial z}\right|_{z=z_0} \right\} dt. \end{aligned} \tag{23}$$

taking in mind that in the plastic hinge the shear is equal to the yield value $T(z_0,t) = T_0(z)$. Indeed, if at the instant $t + dt$ the position of the plastic shear hinge is $z_0 + dz_0$, it must be also $T(z_0 + dz_0, t + dt) = T_0(z_0 + dz_0)$, and $T(z_0 + dz_0, t + dt) = T_0(z_0) + T_0'(z_0)\,dz_0$. The equation (23) in this case is more conveniently written as:

$$\begin{aligned} &\left\{ \mu(z_0)\,\ddot{u}_g(t) + \ddot{v}_1(t)\left.\frac{\partial m_H[z, z_0(t)]}{\partial z}\right|_{z=z_0} \right\} dz_0 + \\ &+ \left\{ m(z_0)\,\dddot{u}_g(t) + \dddot{v}_1(t)\,m_H[z_0, z_0(t)] - \ddot{v}_1(t)\,\dot{z}_0(t)\left.\frac{\partial m_H[z, z_0(t)]}{\partial z}\right|_{z=z_0} \right\} dt = T_0'(z_0)\,dz_0 \end{aligned} \tag{24}$$

and being $\dot{z}_0 = \frac{dz_0}{dt}$, it is:

$$[\mu(z_0)\ddot{u}_g(t) - T_0'(z_0)]\,\dot{z}_0(t) + m(z_0)\ddot{u}_g(t) + \ddot{v}_1(t)m_H[z_0, z_0(t)] = 0\,.$$

By equation (22) the time evolution of the plastic shear hinge is governed by the relation:

$$\dot{z}_0(t) = -\frac{m(z_0)\ddot{u}_g(t) + \ddot{v}_1(t)H(0)m[z_0(t)]}{\mu(z_0)\ddot{u}_g(t) - T_0'(z_0)}. \tag{25}$$

When the plastic hinge moves, residual plastic deformations $\theta_r(z_0,t)$ can be detected in the previous position:

$$\theta_r(z_0,t) = \frac{\dot{v}_1(t)}{\dot{z}_0(t)}$$

and their value do not vary until the plastic hinge forms again at the same position. Hence the acceleration $\ddot{v}(z,t)$ can be determined as functions of the shear:

$$T'(z,t) = T'_{0^+}(z) \Rightarrow \ddot{v}(z,t) = \frac{T'_{0^+}(z)}{\mu(z)} - \ddot{u}_g(t)$$
$$T'(z,t) = T'_{0^-}(z) \Rightarrow \ddot{v}(z,t) = \frac{T'_{0^-}(z)}{\mu(z)} - \ddot{u}_g(t).$$

At the abscissa z the inertial force:

$$q(z) = -\mu(z)[\ddot{u}_g(t) + \int_0^z \ddot{\theta}(x,t)\,dx]$$

allows the total shear written as:

$$T(z,t) = -\int_h^z q(x)\,dx = \ddot{u}_g(t)m(z) + \int_h^z \mu(x)\int_0^x \ddot{\theta}(y,t)\,dy\,dx\,. \tag{26}$$

The (26) can be put after some algebraic manipulations [7] in the form:

$$\begin{aligned}
&[\ddot{u}_g(t) + \int_0^{z_1}\ddot{\theta}(y,t)\,dy - \frac{T_{0^+}(z_1)}{m(z_1)}][\ddot{u}_g(t) + \int_0^{z_1}\ddot{\theta}(y,t)\,dy - \frac{T_{0^-}(z_1)}{m(z_1)}] = 0\\
&\frac{T_{0^-}(z)}{m(z)} < \ddot{u}_g(t) + \int_0^{z_1}\ddot{\theta}(y,t)\,dy < \frac{T_{0^+}(z)}{m(z)} \quad , \quad \forall z > z_1
\end{aligned} \tag{27}$$

According the (27) the plastic deformations stop at the abscissa z_p and cannot propagate upward. The abscissa z_p can be obtained solving a minimum problem independent on time t and on ground acceleration $\ddot{u}_g(t)$:

$$\left.\begin{aligned}
z_{p1} &\rightarrow \frac{T_{0^+}(z_{p1})}{m(z_{p1})} = \min_{z\in(0,h)}\left[\frac{T_{0^+}(z)}{m(z)}\right]\\
z_{p2} &\rightarrow \frac{T_{0^-}(z_{p2})}{m(z_{p2})} = \min_{z\in(0,h)}\left[\frac{T_{0^-}(z)}{m(z)}\right]
\end{aligned}\right\} \Rightarrow \quad z_p = \max(z_{p1}, z_{p2}) \tag{28}$$

when equation (28) is satisfied for $z_p = 0$ the beam response involves only one degree of freedom.

4. Results

A wind turbine tower can be represented by a vertical cantilever beam subjected to harmonic base motion and symmetric yield response of the truss structure, in which the contribute to the total shear force due to the normal force on the diagonal element has been taken into account [7]. The case study is the truss structure whose geometrical properties are reported in [37] and summed in the following:

$$\begin{cases} h = 76.12\,m & (\text{total height of the tower}) \\ \mu(z) = a\,z^2 + b\,z + c & (\text{mass linear density}) \\ \text{with} \quad a = 6.9\times 10^{-2}\,kg\,m^{-3} & e = -30\ kg\,m^{-2},\quad c = 4.904\times 10^{3}\,kg\,m^{-1} \\ \ddot{u}_g(t) = a_0 \sin\omega t & (\text{base motion}) \\ D = 6\ sec & (\text{duration of the time history}) \\ T_0(z) = d\,z^2 + e\,z + f & (\text{yield shear}) \\ \text{with} \quad d = 1.944\times 10^{3}\ Nm^{-2} & e = -518.61\,Nm^{-1},\quad f = 3.18\times 10^{7}\ N \end{cases}$$

The plastic boundary $z_0(t)$ evolves depending on the harmonic forcing time history [38]. The numerical analyses identify a large plastic zone, extended in the range between two sections, the first one near the support (0.5 m) and the second one at 1 m level, both in the first truss bay. Above the plastic sections the remaining part of the tower is in the elastic field. In Figure 3 the time histories of both the plastic shear strain rate at hinge level and the displacement at the tower top are reported.

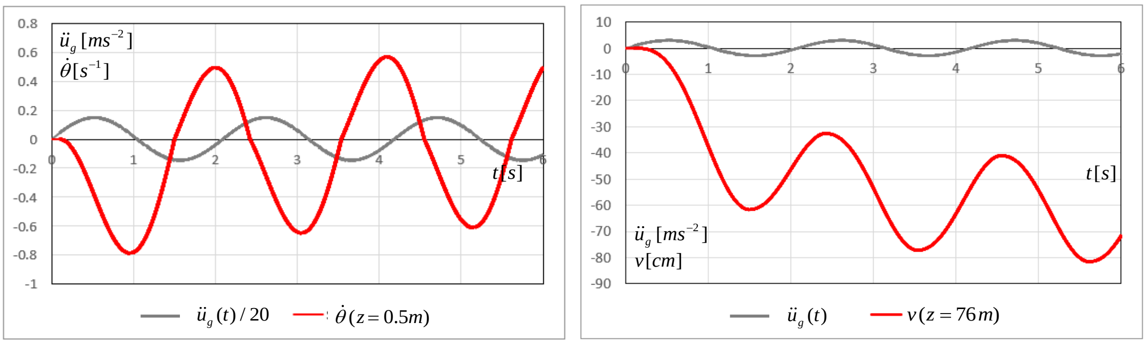

Fig. 3 Time histories of the plastic shear strain rate at the plastic level (left) and displacement at the top of the tower (right) for amplitude $a_0 = 0.2g$ and $f = \omega/2\pi = 0.4775\,Hz$ with $\omega = 3s^{-1}$

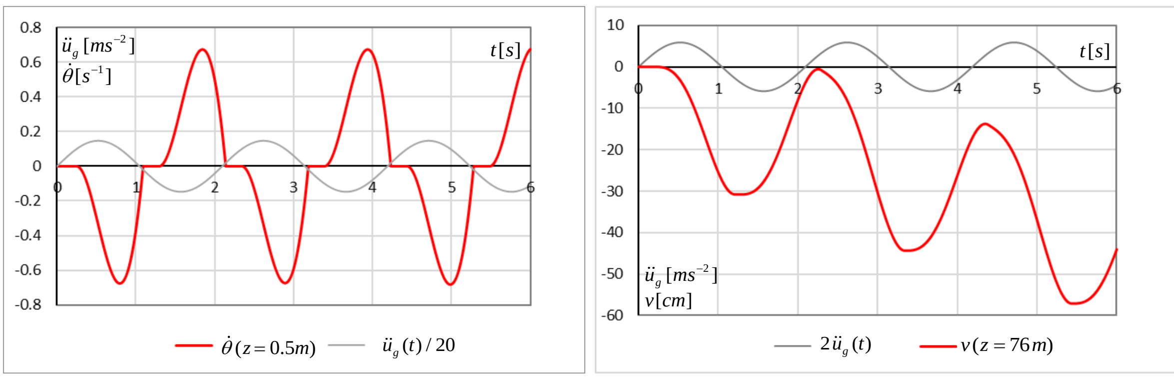

Fig. 4 Time histories of the displacement at the plastic hinge levels (left) and at the top of the tower (right) for amplitude $a_0 = 0.3g$ and $f = \omega/2\pi = 0.4775\,Hz$ with $\omega = 3s^{-1}$

As it can be noted, the shear rate is in both cases a periodic function, ranging in the same numerical interval [39]. The displacement at the top of the tower presents a similar shape, but the maximum displacement value in the examined time interval present an increase of 50%.

5. Conclusions

The behaviour of a truss tower for wind turbines subjected to harmonic ground motion has been analyzed in this paper. The failure is considered due to the formation of shear hinges and the step by step integration method is adopted to calculate the dynamic response of the structure in the whole time domain. This procedure can be efficiently applied when a shear failure is acknowledged, as several collapsed wind towers have shown. The formation of a plastic shear hinge can be easily recognized in the first bay of the truss structure. The model here presented is able to describe the geometrical distribution of shear hinges with a relatively simple procedure.

The proposed procedure provides an efficient representation of the tower post-elastic behaviour and a good estimation of the fundamental response modes with the benefit of low computational efforts and limited number of mechanical parameters. Small modifications allow the analysis of elastoplastic structures with several degree of freedom and generic ground acceleration. The elastoplastic dynamics by means of discretization methods involves in fact significant computational efforts to obtain reliable time histories. With the proposed approach a set of necessary information are provided, among them the localization of damage due to the extension of the plastic front that allows the designer to recognize the segment of tower needing special attention.

6. Aknowledgements

This research was supported by the National Research Project PRIN 2015 *Advanced mechanical modeling of new materials and structures for the solution of 2020 Horizon challenges* (Miur - Ministry of Education, Universities and Research).

7. References

[1] Wen B, Wei S, Wei K, Yang W, Peng Z and Chu F, 2017. Power fluctuation and power loss of wind turbines due to wind shear and tower shadow. *Front. Mech. Eng.*, 12(3): 321-332.

[2] Chen S, Li Q, Liu Y, Xia J and Xue Z, 2011. Dynamic elastoplastic analysis using the meshless local natural neighbor interpolation method. *Int. J. Comp. Meth.*, 8(3): 463-481.

[3] Bonavolontà C, Peluso G, Valentino M, De Iorio A and Penta F, 2009. Detection of magnetomechanical effect in structural steel using SQUIDs and flux-gate sensors. *J. Supercond. Nov. Magn.*, 22(8): 833-839.

[4] Schubak RB, Anderson DL and Olson MD. Simplified dynamic analysis of rigid-plastic beams. *Int. J. Impact Eng.,* 1989, 8(1): 27-42.

[5] Gesualdo A and Monaco M, 2015. Constitutive behaviour of quasi-brittle materials with anisotropic friction. *Lat. Am. J. Solids Struct.*, 12(4): 695–710.

[6] Fraldi M, Gesualdo A and Guarracino F, 2014. Influence of actual plastic hinge placement on the behavior of ductile frames. *J. Zhejiang Univ. Sci. A*, 15(7): 482-495.

[7] Cennamo C, Gesualdo A and Monaco M, 2017. Shear plastic constitutive behaviour for near-fault ground motion, *J. Eng. Mech. ASCE*, 143(9): 04017086.

[8] Málaga-Chuquitaype C, Elghazouli AY and Bento R, 2009. Rigid-plastic models for the seismic design and assessment of steel framed structures. *Earthq. Eng. Struct. Dyn.*, 38(14): 1609-1630.

[9] Nonaka T, 1977. Shear and Bending Response of a Rigid-Plastic Beam to Blast-Type Loading. *Ing. Arch.*, 46(1): 35-52.

[10] Li QM and Meng H, 2002. Pulse loading shape e effects on pressure–impulse diagram of an elastic–plastic, single-degree-of-freedom structural model. *Int. J. Mech. Sci.*, 2002, 44(9): 1985-1998.

[11] Symonds PS and Fleming WTJ, 1984. Parkes revisited: on rigid-plastic and elastic-plastic dynamic structural analysis. *Int. J. Impact Eng.*, 2(1): 1-36.

[12] Liang MT, Lee BJ and Yang SS, 1997. On the rigid ideally plastic deformation of cantilever beam subjected to tip impact. *J. Mar. Sci. Technol.*, 5(1): 39-46.

[13] Lloyd Smith D and Sahlit CL, 1991. Dynamic response of pulse loaded structures as a linear complementarity problem. *Eng. Optimiz.*, 18(1-3): 23-41.

[14] Khan A, Smith DL and Izzuddin BA, 2013. Investigation of rigid-plastic beams subjected to impact using linear complementarity. *Eng. Struct.*, 50: 137-148.

[15] Wang RZ, Tsai KC and Lin BZ, 2011. Extremely large displacement dynamic analysis of elastic–plastic plane frames. *Earthq. Eng. Struct. Dyn.*, 40(13): 1515-1533.

[16] Li QM, 2000. Continuity conditions at bending and shearing interfaces of rigid, perfectly plastic structural elements. *Int. J. Solids Struct.*, 37(27): 3651-3665.

[17] Chierchiello G, Gesualdo A, Iannuzzo A, Monaco M and Savino MT, 2015. Structural modeling and conservation of single columns in archaeological areas. *In: Proc. 14th Int. Forum "Le vie dei mercanti"*, C. Gambardella, ed., Vol. 56, La Scuola di Pitagora Editrice, Napoli, Italy, 2012-2020.

[18] Gesualdo A, Iannuzzo A, Penta F and Pucillo GP, 2017b. Homogenization of a Vierendeel girder with elastic joints into an equivalent polar beam. *J. Mech. Mater. Struct.*, 12(4): 485-504.

[19] Penta F, Monaco M, Pucillo GP and Gesualdo A, 2017. Periodic beam-like structures homogenization by transfer matrix eigen-analysis: A direct approach. *Mech. Res. Commun.*, 85: 81-88.

[20] Paglietti A and Porcu MC, 2001. Rigid-plastic approximation to predict plastic motion under strong earthquakes. *Earthq. Eng. Struct. Dyn.*, 30(1): 115-126.

[21] Ren YT, Qiu XM and Yu TX, 2014. The sensitivity analysis of a geometrically unstable structure under various pulse loading. *Int. J. Impact Eng.*, 70: 62-72.

[22] Monaco M, Guadagnuolo M and Gesualdo A, 2014. The role of friction in the seismic risk mitigation of freestanding art objects. *Nat. Hazards*, 73(2), 389–402.

[23] Gesualdo A, Iannuzzo A, Monaco M and Penta, F, 2017a. Rocking of a rigid block freestanding on a flat pedestal. *J. Zhejiang Univ. Sc. A*, 19(5), 331-345.

[24] Vassiliou MS and Makris N, 2011. Estimating Time Scales and Length Scales in Pulselike Earthquake Acceleration Records with Wavelet Analysis. *B. Seismol. Soc. Am.*, 101(2): 596-618.

[25] Makris N and Vassiliou MS, 2013. Planar rocking response and stability analysis of an array of free-standing columns capped with a freely supported rigid beam. *Earthq. Eng. Struct. Dyn.*, 42(3): 431–449.

[26] Li S, Zhai C and Xie LL, 2009. Analysis on response of dynamic systems to pulse sequences excitation. *Int. J. Adv. Struct. Eng.*, 1(1), 3-15.

[27] Mylonakis G and Voyagaki E, 2006. Yielding oscillator subjected to simple pulse waveforms: numerical analysis and closed-form solutions. *Earthq. Eng. Struct. Dyn.*, 35(15): 1949-1974.

[28] Gesualdo A, Iannuzzo A, Monaco M and Savino MT, 2014. Dynamic analysis of freestanding rigid blocks, in: *B.H.V. Topping, P. Iványi (Eds.), Civil-Comp Proc. 12th Int. Conf. Computational structures technology*, Civil Comp Press, Kippen, Stirlingshire, UK, 106.

[29] Gesualdo A, Iannuzzo A, Modano M and Monaco M, 2017. Dynamic behaviour of two stacked rigid blocks, in: *AIMETA 2017 – Proc. 23rd Conf. Italian Association of Theoretical and Applied Mechanics*, 4: 778-791.

[30] Mavroeidis GP and Papageorgiou AS, 2003. A mathematical representation of near-fault ground motions. *B. Seismol. Soc. Am.*, 93(3), 1099-1131.

[31] Augusti G, 1970. Rigid-plastic structures subject to dynamic loads. *Meccanica*, 5(2): 74-84.

[32] Bergamasco I, Gesualdo A, Iannuzzo A and Monaco M, 2018. An integrated approach to the conservation of the roofing structures in the Pompeian Domus. *J. Cult. Herit.*, 31: 141-151.

[33] Guadagnuolo M and Monaco M, 2009. Out of plane behaviour of unreinforced masonry walls, in: *F.M. Mazzolani (Ed.), Protection of Historical Buildings*, CRC Press, Taylor & Francis Group, London, New York, 2: 1177–1180.

[34] Martin JB, 1981. The determination of mode shapes for dynamically loaded rigid-plastic structures. *Meccanica*, 16(1): 42-45.

[35] Martin JB, 1965. A displacement bound principle for inelastic continua subjected to certain classes of dynamic loading. *J. Appl. Mech.*, 32(1): 1-6.

[36] Gesualdo A, Iannuzzo A, Minutolo V and Monaco M, 2018. Rocking of freestanding objects: theoretical and experimental comparisons, *J. Theor. App. Mech-Pol.*, 56(4).

[37] Magalhaes Junior PAA, Rios IG, Ferreira TS, de Andrade Junior AG, de Carvalho Filho OA and Magalhaes CA, 2014. Structural analysis and structural optimization of self-supporting truss towers to support a large wind turbine, *Int. J. Optim. Civil Eng.*, 4(3):341-359.

[38] Gesualdo A, Iannuzzo A, Penta F and Monaco M, 2019. Nonlinear dynamics of a wind turbine tower, *Front. Mech. Eng.*, doi: https://doi.org/10.1007/s11465-019-0524-y (in press)

[39] Calderoni B, Giubileo C and De Martino A, 2006. Assessment of hysteretic cyclic behaviour of plastic hinge in cold-formed steel beams. *Proc. 5th Int. Conf. on behaviour of steel structures in seismic areas, STESSA 2006*, 185-190.